A Simplified Model of Low Reynolds Number, immiscible, Gas-Liquid Flow and Heat Transfer in Porous Media (Numerical Solution with Experimental Validation)

Gamal B. Abdelaziz (gbedair@gmail.com)
Suez University
M. Abdelgaleel
Suez University
Z.M. Omara
Kafrelsheikh University
A. S. Abdullah
Prince Sattam bin Abdulaziz University
Emad M.S. El-Said
Fayoum University
Swellam W. Sharshir
Kafrelsheikh University
Ashraf Mimi Elsaid
Helwan University

Research Article

Keywords: Two phase flow, Porous media, Immiscible, Concurrent, Darcy model

Posted Date: February 22nd, 2021

DOI: https://doi.org/10.21203/rs.3.rs-260636/v1

A Simplified Model of Low Reynolds Number, immiscible, Gas-Liquid Flow and Heat Transfer in Porous Media (Numerical Solution with Experimental Validation)

Gamal B. Abdelaziz[1,*], M. Abdelgaleel[1], Z.M. Omara[2], A. S. Abdullah[3,4], Emad M.S. El-Said[5], Swellam W. Sharshir[2], Ashraf Mimi Elsaid[6,*]

1 Mechanical Department, Faculty of Technology and Education, Suez University, Egypt

2 Mechanical Engineering Department, Faculty of Engineering, Kafrelsheikh University, Egypt

3 Mechanical Engineering Dept., College of Engineering, Prince Sattam bin Abdulaziz University, KSA

4 Mechanical Power Engineering Department, Faculty of Engineering, Tanta University, Tanta, Egypt

5 Mechanical Engineering Department, Faculty of Engineering, Fayoum University, Fayoum, Egypt

6 RHVAC Technology Department, Faculty of Technology and Education, Helwan University, Cairo 11282, Egypt.

- Corresponding Author

Abstract:

This study investigates the thermal-hydraulic characteristics of immiscible two-phase flow (gas/liquid) and heat transfer through porous media. This research topic is interested among others in trickle bed reactors, the reservoirs production of oil, and the science of the earth. Characteristics of two-phase concurrent flow with heat transfer through a vertical, cylindrical, and homogeneous porous medium were investigated both numerically and experimentally. A generalized Darcy model for each phase is applied to derive the momentum equations of a two-phase mixture by appending some constitutive relations. Gravity force is considered through investigation.

To promote the system energy equation, the energy equation of solid matrix for each phase are deemed. The test section is exposed to a constant wall temperature after filled with spherical beads. Numerical solution of the model is achieved by the finite volume method. The numerical procedure is generalized such that it can be reduced and applied to single phase flow model. The numerical results are acquired according to, air/water downward flow, spherical beads, ratio of particle diameter to pipe radius D=0.412, porosity φ=0.396, $0.01 \leq Re \leq 500$, water to air volume ratio $0 \leq W/A \leq \infty$, and saturation ratio $0 \leq S_1 \leq 1$.

To validate this model an experimental test rig is designed and constructed, and the corresponding numerical results are compared with its results. Also, the numerical results were compared with other available numerical results. The comparisons show good agreement and validate the numerical model. One of the important results reveals that the heat transfer is influenced by two main parameters; saturation ratios of the two fluids; S_1 and S_2, and the mixture Reynolds number Re. The thermal entry length is directly dependent on Re, S_1, and the thermofluid properties of the fluids. A modified empirical correlation for the entrance length; $X_e = 0.1\ Re.Pr.R_m$ is predicted, where $R_m = R_m(S_1, S_2, \rho_1, \rho_2, c_1, c_2)$. The predicted correlation is verified by comparing with the supposed correlation of Poulikakos and Ranken (1987) and El-Kady (1997) for a single-phase flow; $X_e/Pr = 0.1\ Re$.

Keywords: Two phase flow, Porous media, Immiscible, Concurrent, Darcy model.

I. Introduction

Two phase flows through porous media are known to occur in several industrially relevant branches such as in oil and gas production, trickle bed reactors, geothermal engineering, cooling of debris following accidents in nuclear power plants and many other applications. Fundamental studies related to single-phase flow and thermal convection in porous media have increased significantly during recent years. Several studies concerning with single-phase flow and heat transfer through porous media have been reported. Among them, Poulikakkos and Renken [1] approached a numerical simulation to analyze the problem of forced convection of fluid flow in a channel. The channel was filled with a fluid-saturated by a porous medium. The influence of variables of porosity, flow inertia, and Brinkman friction was examined. The dynamics of fluid flow through porous media was performed by Nield and Bejan [2] using the Darcy flow model. The study aimed to develop the heat transfer through a fluid-saturated porous medium utilizing the principles of fluid mechanics. El Kady [3] discussed functionally and historically the forms of governing equations that characterize the fluid flow behavior and convective heat transfer through porous media. Single phase forced convection heat flow in a cylindrical packed bed with either a uniform wall heat flux or a constant wall temperature was examined numerically for both the developing and fully developed regions by El Kady [4,5]. Besides the energy equation, the generalized form of the momentum equation including the non-Darcian effects such as the inertia, viscous forces, and the porosity variation was considered. Non-Newtonian effects and fluid flow and heat transfer characteristics were presented by El Kady et al [6].

The literature studies concern the two-phase flow and heat transfer in porous media can be classified into experimental studies and modeling and formulation studies. The first experimental attempt to study this problem was by Larkins [7]. The simultaneous vertical downward flow of liquids and gases over a fixed packed bed was studied experimentally. Rao et al [8], Saez et al [9], and Sai and Varma [10] focused experimentally, the hydrodynamics of concurrent gas-liquid flow in packed beds. A formulation by Wang and Beckerman [11] was approached for a two-phase of constituents of a binary mixture flow model. The Darcy model with the effect of gravity is formulated besides the energy equation while no results were presented. Other macroscopic modeling studies were performed by Rao et al [12], Saez et al [13] and Hilfer [14]. A review by Carbonell [15] performed different theories of multiphase flow models in packed beds of chemical reactor

design. Likewise, summaries of the conventional multiphase flow model (MFM) and a more recent multiphase mixture model (MMM) were approached by V.Starikovicius [16]. P. J. Binning [17] presented a two-dimensional model of unsaturated zone multiphase air water flow and contaminant transport. The incompressible multiphase flow equations were written in two forms: with the two individual phase pressures or using the global pressure saturation approach of petroleum engineering. Coarse scale equations describing two-phase flow in heterogeneous reservoirs are developed by L. J. Durlofsky [18]. The volume-averaged equations were simplified and applied to the direct solution of a model coarse scale problem. The investigations of both T. W. Patzek and R. Juanes [19] and C. M. Marle [20] intended a three-phase fluid flow of one-dimensional immiscible equations with gravity effect, in the limit of negligible capillarity. Their main study results concluded that a Darcy flow model was insufficient to express all the physics principles of co-current three-phase displacements through reservoirs. As a result of not computing some physical phenomena in Darcy's equation, especially with multi-phase flows in porous media, a multifaceted mathematical approach has been described to derive deterministic conservation equations on the length scale with the realization of thermodynamic constraints by Julia C. Muccino et al. [21]. The study found a set of equilibrium equations that presumed a framework for determining the assumptions inherent in a multiphase flow model. The same factors were investigated numerically by J. Niessner and S. M. Hassanizadeh [22] and found that the modified model compared to the standard model required an additional physical process such as hysteresis. A 2D numerical model of a porous medium with an incompressible fluid with non-zero Reynolds number was simulated by Sergio Rojas and Joel Koplik [23]. A random array of square cross-section cylinders was utilized. The manifested results found that a transition Darcy from linear flow field at evanescence Re to a cubic transitional regime at low Re, and then a quadratic Forchheimer when Re=0(1). Tore I. Bjørnarå et al. [24] studied 2D numerical model by different types of equations that describe two-phase flow in porous media using the finite element method. These equations consist of mass balances, partial differential equations for accumulation, transport, and injection/production of the phases. Other auxiliary equations were applied such as hydraulic properties, coupling the phases through the system. The test results predicted that the fractional flow formulation was the fastest and most robust formulation. A thesis of Jennifer Niessner [25] dealt with thermodynamically consistent modeling of a two-stage flow in porous media to optimize the interfaces of the conservation equations for mass, momentum, energy, and entropy of the phases and interfaces through the system. The

dissertation discussed the criteria for obtaining important parameters and the constitutive relationships of the interfacial-area-based model experimentally or numerically and was considered a qualitative feature of the model. The disadvantage of this model compared to the classic model was that it takes longer for complex dynamic computing. An efficient simulating numerical model with complex interface motion and irregular solid boundaries of multiphase flow in porous media was done by Ali Q. Raeini et al. [26]. Navier Stokes equations were approached using a finite volume method, whereas the VOF method was utilized the location of interfaces. A model of semi-sharp surface force was utilized to obtain the capillary force at low capillary numbers. The result indicated that the potential of the method to predict multiphase flow processes was suitable. Bertrand Lagree [27] numerically simulated a multiphase flow through a porous media by VOF scheme with Gerris code. The paper was conducted a simulation of Saffman-Taylor fingering by the analysis of waterflooding experiments of extra-heavy oils in quasi-2D square slab geometries of Bentheimer sandstone. The numerical model was verified with an available data in literature. At late times, the area of the resulting pattern varies as the length of, with different values for finite or infinite viscosity contrasts. a review of the transport flow through porous media was conducted by Michel Quintard. Simple heat conduction in porous media was a problem that needed a review. Various variants were discussed through a review as, volume averaging, homogenization, stochastic approaches, and length-scale ratios. The extensions to more complicated problems of heat transfer in porous media, characterized by various couplings between transport problems were discussed. Creeping two-phase flows through porous media were carried out numerically by Sylvain Pasquier et al. [29] utilizing the Buckley-Leverett theory. The investigation was conducted for different couples of fluids and closure relations of the effective parameters. The obtained results manifested that the increment of momentum exchange through two-phase flow could be done by the permeability of porous media. The finding was constrained to the effect of the interfaces between fluid/fluid as much like the interfaces of solid/fluid. Another one-dimensional numerical model was proposed by Yangyang Qiao et al. [30] of two-phase flow on porous media. The fluid/fluid drag force and internal viscosity effects were considered in momentum balance equations as fluid-solid interfaces. The result demonstrated the differences and similarities of a formulation based on Darcy velocity and interstitial velocity in viscous terms. Lili Wang et al. [31] experimentally studied the flow behaviors through porous media with a lower Reynolds number. The experimentation was conducted a sand column-based laboratory filtration process. The media were contained two silts samples with two modes of silty sand and medium sand. A constant

hydraulic head was an important factor that influenced the flow behaviors through porous media. Hybrid of solid/free media through porous matrices in two-phase flow was simulated numerically by an approach of multiphase Darcy-Brinkman. A numerical model of Francisco J. Carrillo et al. [32] was utilized a set of partial differential equations (PDE) to predict flow behaviors in both regions and scales. The model combined a Navier-Stokes VOF for the interface of solid/free and the multiphase Darcy equations in a porous interface. The solver versatility was depicted utilizing applications of two-phase flow in wave interaction with a porous coastal barrier and a fractured porous matrix. An attempt to simulate a compressible and immiscible three-phase flow through porous media was discussed by Yangyang Qiao and Steinar Evje [33]. The main idea was to subrogate Darcy's law with momentum balance equations for viscous coupling effects by fluid/fluid regime terms from the model of Qiao et al. [34] on a water/oil mixture. Compressible and incompressible model similarities and differences were spotted with the fluid/fluid interface behaviors. Aerosol droplets cause a threat to human health that leads to death and are removed from the air by using face masks. It was a challenge by André Baumann et al. [35]. Due to the complexity of two-phase flow processes, nano CT scans and micro-scale simulations of a macro-scale approach with the two-phase flow through fibrous filters were experimentally and numerically conducted to predict a pressure loss and filtration efficiency. Numerous complex micro-scale phenomena as droplet coalescence, breakup, or film flow occur before the macro-scale residual saturation was remarked. Mays and Zena [36] experimentally studied three different porous media in a container with width 0.2m w, height 0.2 m, and depth of 0.27 m under a heat flux of 500 W/m^2. The container sides were isolated whilst the convection heat transfer coefficient of the container top was fixed at 10 W/m. The materials of porous media were aluminum, Al_2O_3, glass, and silica/sand. The manifested findings proved that the maximum velocity and pressure were obtained by glass and water porous media. Moreover, aluminum and water porous media accorded the minimum velocity, pressure, and temperature. Due to the complicated transport phenomena involved, the two-phase flow and heat transport in porous media remain poorly understood. The purpose of this study is to present a complete view about immiscible, gas-liquid flow and heat transfer through porous media. Conservation laws for each phase considering steady, downward two-phase flow through porous media are mathematically described. The governing macroscopic equations of this model are derived considering the gravity effect in the generalized Darcy's law. A numerical scheme for the solution of the two-phase mixture model under consideration was introduced based on finite volume technique. Experimental work is presented to validate this model.

II. Definitions:

Porosity:

The average porosity of a block in a porous medium is the ratio of the pore space to the bulk volume of the block.

$$\varphi = \frac{Vp}{Vt} \tag{1}$$

For two phase flow in porous media,

$$\varphi = \frac{V_1 + V_2}{Vt} \tag{2}$$

$$V_t = V_1 + V_2 + V_3 \tag{3}$$

Where V_1, V_2, and V_3 are the volumes occupied by fluid 1, 2 and solid matrix, respectively.

The porosity can be divided into two parts: φ_1 and φ_2 for fluid 1 and fluid 2. Thus.

$$\varphi_1 = \frac{V_1}{Vt}, \quad \varphi_2 = \frac{V_2}{Vt}, \quad \text{and} \quad \varphi = \varphi_1 + \varphi_2 \tag{4}$$

Saturation:

The average saturation of fluid 1 (S_1) is defined as the ratio of the volume occupied by this fluid to the volume of voids in the medium.

$$S_1 = \frac{V_1}{V_1 + V_2}, \quad S2 = \frac{V_2}{V_1 + V_2} \quad \text{and} \quad S_1 + S_2 = 1 \tag{5}$$

Permeability

Darcy had defined the permeability as the ability of fluid to flow through the porous material by an applied pressure gradient; it is the fluid conductivity. Let us imagine this experiment: two fluids 1,2 entering a porous block and leaving at the exit section spacing L from the inlet section. Δp is the pressure gradient along the distance L. Considering steady flow and using Darcy law.

$$u_1 = -\frac{K_1}{\mu_1}.\frac{\Delta p}{L} \quad \text{and} \quad u_2 = -\frac{K_2}{\mu_2}.\frac{\Delta p}{L} \tag{6}$$

where K_1 and K_2 are the effective permeabilities of fluids 1 and 2 respectively and obviously depend on the nature of the medium under consideration and saturation of the fluid.

Relative permeabilities:

Relative permeability of a fluid is the ratio of its effective permeability to the medium permeability, K.

$$K_{r1}=K_1/K \quad \text{and} \quad K_{r2}=K_2/K \tag{7}$$

Relative permeabilities are functions of saturation of each fluid.

$$K_{r1}=K_{r1}(S_1) \quad \text{and} \quad K_{r2}=K_{r2}(S_2) \tag{8}$$

The widely used functions of K_{r1} and K_{r2} are:

$$K_{r1} = (S_1)^n \quad \text{and} \quad K_{r2} = (1-S_1)^n \tag{9}$$

- Linear functions; n=1; are usually employed for air-water systems.
- Square functions; n=2; are suitable for petroleum engineering; oil water system.
- Cubic forms; n=3; are widely used in nuclear safety engineering.

Bejan [2] concluded that satisfactory results have been reported when use has been made of a simple linear relationship namely:

$$K_{r1} = S_1 \quad \text{and } K_{r2} = 1- S_1. \tag{10}$$

Mixture density:

The mixture density is defined as:

$$\rho = \rho_1 S_1 + \rho_2 S_2 = \rho_1 S_1 + \rho_2 (1- S_1) \tag{11}$$

Mixture specific heat:

The mixture specific heat is defined as a function of individual specific heat of each phase as follows:

$$c = c_1 S_1 + c_2 (1- S_1) \tag{12}$$

Mixture velocity:

u_1, u_2, and u are the Darcian velocities of the fluid 1, fluid 2, and mixture respectively (based on the total cross section area);

$$u = (\rho_1 u_1 + \rho_2 u_2)/\rho \tag{13}$$

Effective thermal conductivity of the medium:

The effective thermal conductivity of two phase flow through a porous medium with porosity φ and thermal conductivity k_1, k_2, and k_3 for fluid 1, fluid 2, and solid matrix respectively; is defined as follows: $k_{ef} = (1-\varphi)\, k_3 + \varphi\, (k_1 S_1 + k_2 S_2)$ (14)

III. Mathematical Formulation:

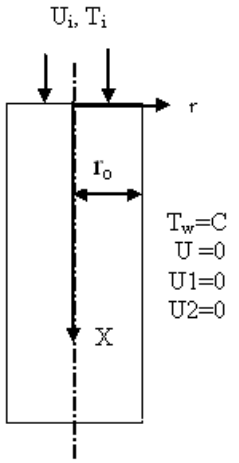

Fig.1. Physical model, coordinate system and boundaries

A schematic for the physical configuration is shown in Fig.1. It is assumed that the two-phase flow through the porous medium is steady, concurrent, and downward the two fluids are immiscible and incompressible, the individual fluid phases always remain continuous, the solid matrix is incompressible and homogeneous. Gravity forces are considered, and capillary pressure is neglected. The saturation of each fluid is constant along the test section. No mass sources or heat sources are considered.

The test section is a cylindrical pipe filled with porous medium and is exposed to constant wall temperature T_w on the outer surface. A porous medium consisting of packed spheres is used to illustrate the results. It is also assumed that the two fluids and the solid matrix are in thermal equilibrium.

The thermo physical properties of the solid matrix and the two phases such as the viscosity, thermal conductivity, and effective thermal diffusivity are assumed to be constant. Consider the simultaneous flow of the two phases denoted as liquid (subscripted 1) and gas (subscripted 2) through a porous solid matrix (subscripted 3) while the mixture properties are not subscripted. The accepted and widely used macroscopic continuity equations are based on conservation of each fluid.

$$\nabla.\rho_1 u_1=0, \quad \nabla.\rho_2 u_2=0 \text{ and } \quad \nabla.(\rho_1 u_1+\rho_2 u_2)=0 \tag{15}$$

The development of momentum equation for two phase flow through porous media can be obtained from the Darcy flow model for each phase by some algebraic manipulation. If capillary pressure is neglected, the Darcy flow model which reflecting relationships of flow velocities with phase pressure can be derived as follows:

$$u_1 = -\frac{K_1}{\mu_1}.(\nabla p - \rho_1 g) \quad \text{and} \quad u_2 = -\frac{K_2}{\mu_2}.(\nabla p - \rho_2 g) \tag{16}$$

$$K_1 = K\, K_{r1}, \text{ and } \quad K_2 = K\, K_{r2}$$

where K is the absolute permeability of the porous medium, K_1 and K_2 are the permeabilities of fluid 1 and 2 in the porous medium respectively, K_{r1} and K_{r2} are the relative permeabilities of phases 1 and 2, respectively.

Adding the two equations.

$$\rho u = -K\left[\frac{K_{r1}}{\nu_1}.(\nabla p - \rho_1 g) + \frac{K_{r2}}{\nu_2}.(\nabla p - \rho_2 g)\right]$$

$$= -K\left[\left(\frac{K_{r1}}{\nu_1} + \frac{K_{r2}}{\nu_2}\right).\nabla p - g\left(\frac{\rho_1 K_{r1}}{\nu_1} + \frac{\rho_2 K_{r2}}{\nu_2}\right)\right]$$

$$= \frac{-K}{\nu}\left[\nabla p - g(\lambda_1\rho_1 + \lambda_2\rho_2)\right]$$

$$= \frac{-K}{\nu}\left[\nabla p - g\rho_k\right]$$

$$u = \frac{-K}{\mu}(\nabla p - \rho_k g) \tag{17}$$

Where ν is the kinematic viscosity of the mixture; $\nu = \dfrac{1}{\dfrac{K_{r1}}{\nu_1} + \dfrac{K_{r2}}{\nu_2}}$ (18)

λ_1 and λ_2 are the relative mobilities of phases 1 and 2, respectively,

$$\lambda_1 = \frac{\nu K_{r1}}{\nu_1} \quad \text{and} \quad \lambda_2 = \frac{\nu K_{r2}}{\nu_2} \tag{19}$$

The introduced new mixture density ρ_k is called the kinematic mixture density. It acquires its name because of its dependence of the relative mobilities of the phases.

The total energy conservation equation for a combined solid matrix and two-phase mixture system is required to determine the temperature field. By assuming that local thermal equilibrium prevails among the solid matrix, gas phase and liquid phase (i.e., $T=T_1=T_2=T_3$) and for steady conditions without evaporation and with no heat sources.

$$\nabla.(\rho_1 u_1 h_1 + \rho_2 u_2 h_2) = \nabla.(k_{ef}.\nabla T) \tag{20}$$

where k_e is the effective thermal conductivity of the combined three phase system,

$k_{ef} = (1-\varphi)\, k_3 + \varphi\,(S_1 k_1 + S_2 k_2)$,

h_1 and h_2 are the enthalpies of phase 1 and phase 2, respectively.

Assuming constant properties of phases, equation (15) becomes:

$$(\rho_1 u_1 c_1 + \rho_2 u_2 c_2)\frac{\partial T}{\partial x} = K_e.\left(\frac{\partial^2 T}{\partial x^2} + \frac{\partial^2 T}{\partial r^2} + \frac{1}{r}.\frac{\partial T}{\partial r}\right) \tag{21}$$

Where c_1 and c_2 are the heat capacities of phase 1 and phase 2, respectively.

In this model, the velocity of each fluid is assumed to be uniform and consequently the mixture velocity. At the outer radius, there is a constant wall temperature T_w. At the inlet of test section, x=0, the fluid has a uniform velocity ui and uniform temperature T_i, i.e., the following boundary conditions are applied:

At $r=r_o$ $T=T_w$, At $x=0$ $T=T_i$

To nondimensionalize the governing equations (15), (17), and (21), the following scaling are used: $R=r/r_o$, $D=d/r_o$, $X=x/r_o$, $U_1=u_1/u_i$, $U_2=u_2/u_i$, $U=u/u_i$, and $\partial T=(T_w-T_i)\,\partial\theta$

$$\theta=\frac{(T-T_i)}{(T_w-T_i)}$$

The steady state dimensionless form of the governing equations now becomes,

$$\nabla.U=0 \tag{22}$$

$$U.\mathrm{Re}=\mathrm{Da}\,.\,(B+Ga) \tag{23}$$

$$(Rc_1U_1+Rc_2U_2)\mathrm{Re}.\mathrm{Pr}\frac{\partial\theta}{\partial X}=\frac{\partial^2\theta}{\partial R^2}+\frac{1}{R}.\frac{\partial\theta}{\partial R}$$

$$Rm.\mathrm{Re}.\mathrm{Pr}\frac{\partial\theta}{\partial X}=\frac{\partial^2\theta}{\partial R^2}+\frac{1}{R}.\frac{\partial\theta}{\partial R} \tag{24}$$

where: Reynolds number $\mathrm{Re}=u_i.r_o/\nu$, Darcy number $Da=K/r_o^2$,

Galileo number $Ga=\frac{g\rho\rho_k r_o^3}{\mu^2}$, dimensionless pressure drop $B=-(r_o^3/\rho\nu^2).\partial P/\partial x$, Prandtl number $\mathrm{Pr}=\nu/\alpha e$, $Rc_1=\rho_1c_1/\rho c$, $Rc_2=\rho_2c_2/\rho c$, and $R_m=Rc_1.U_1+Rc_2.U_2$.

IV. Fluid Flow and Heat Transfer Characteristics:

The flow through the porous duct experiences in general the boundary frictional drag "f_v", a bulk frictional drag induced by the solid matrix (designed as Darcy's pressure drop) "f_D", the drag induced by gravity effect "f_g", and a flow inertia drag "f_i" induced by the solid matrix at high velocities (designed as Forschheimer's form drag) [5,6]. Under the present assumptions, f_v and f_i are neglected and the remaining two factors can be defined after changing the variables to the present notations and definitions as follows:

$$f_D=\frac{\mu u_m\varphi}{K}.\frac{r_o}{2}\Big/\frac{1}{2}\rho u_m^2 \tag{25}$$

where the total bulk drag can be calculated from the experimentally measured data as follows:

$$f_t=-\frac{\partial p}{\partial x}.\frac{r_o}{2}\Big/\frac{1}{2}\rho u_m^2 \tag{26}$$

Equation (25) can be written as a function of the dimensionless parameters as:

$$f_D=\varphi/Da.\mathrm{Re} \tag{27}$$

The heat transfer characteristics in a channel flow are indicated by the Nusselt number and the thermal entrance length which characterize the developing flow. Nusselt number at the wall can be derived in the dimensionless form as follows:

$$Nu = \frac{\left|\frac{\partial T}{\partial r}\right|_w . r_o}{T_w - T_m} = \frac{\left|\frac{\partial \theta}{\partial R}\right|_w}{\theta_w - \theta_m} \tag{28}$$

Where the subscript w refers to the wall of the pipe, T_m is the mean fluid temperature defined in a manner like that for classical fluid duct flows:

$$T_m = \int_0^{ro} \rho u T r \, dr \Big/ \int_0^{ro} \rho u r \, dr \tag{29}$$

The average Nusselt number over the total length of the test section can be calculated as follows.

$$Nu_a = \frac{1}{L}\int_0^L Nu.dx \tag{30}$$

The mean temperature cannot be measured experimentally as calculated in Eq. 29, thus; to compare the numerically calculated Nusselt number with the experimentally measured one, another value of Nusselt number symboled Nu^* is introduced. In which the mean temperature is considered as the arithmetic mean value of input and exit temperatures.

$$Nu^* = \frac{\left|\frac{\partial \theta}{\partial R}\right|_w}{\theta_w - \theta_m} = \frac{\left|\frac{\partial \theta}{\partial R}\right|_w}{1 - 0.5\theta_e} \tag{31}$$

The thermal entrance length X_e is defined as the distance between the entrance of the pipe and the point at which the mean fluid temperature θ_m and Nusselt number Nu become independent of the x-location.

V. Numerical Formulation:

Because the present configuration is symmetrical with respect to the centerline, only half of the channel needs to be considered. The finite volume method with variable grid step in X direction is employed. The R domain is discritized into 201 grid points to get an accurate resolution of the important near wall region. A very fine grid size in the X direction near the channel inlet and coarser downstream is used. The grid size at the inlet is 0.0001 and increases gradually in the downstream direction by a multiplier factor 1.01. This is done to capture the steep changes in the temperature field near the entrance. The energy equation was

transformed into algebraic finite volume equations by integration following the procedure developed by Patankar [37] and Versteeg [38]. It can be solved considering constant velocity field to get the temperature distribution. A system of tridiagonal algebraic equations for the nodal temperature at any given X position is obtained. Once the temperature profile at each X position is known, the local Nusselt numbed is determined from equation (20). When the mean fluid temperature θ_m and Nusselt number Nu become independent of the x-location a thermally fully developed flow is assumed and the entrance length is obtained.

VI. Experimental work:

To validate the mathematical and numerical model, an experimental work is done. Schematic layout of the experimental test rig is shown in Fig. (2), in which the test section (12) is loaded by means of steel stand, which permits to change the porous medium easily. Water was pumped from a 200 L tank (1) at 5.5 m height to the midpoint of the test section. It flows through a control valve (3) to a rotameter (6), which measures the flow rate of water, J. W. Dally [39]. Air was drawn from a compressor (15) through a control valve (16) to an air test section (17) of 55 cm length and 3.75 cm diameter. Air velocity and temperature are measured by means of a hot wire anemometer (18), which is located at the end of the air test section. A definite mass flow rate of each air and water were mixed before entering the test section to flow through the porous medium inside the test section. The temperature of outer wall of the test section is maintained constant by means of passing a saturated steam through an outer annulus from an electric boiler. Temperatures were measured by copper-constantan type-J thermocouples (4), which are attached to digital temperature recorder type YOKOGAWA (5) with scale division of 0.1 °C and 24 channels. Four pressure gauges (7) were attached at four levels to measure the pressure at each section along the length of test section.

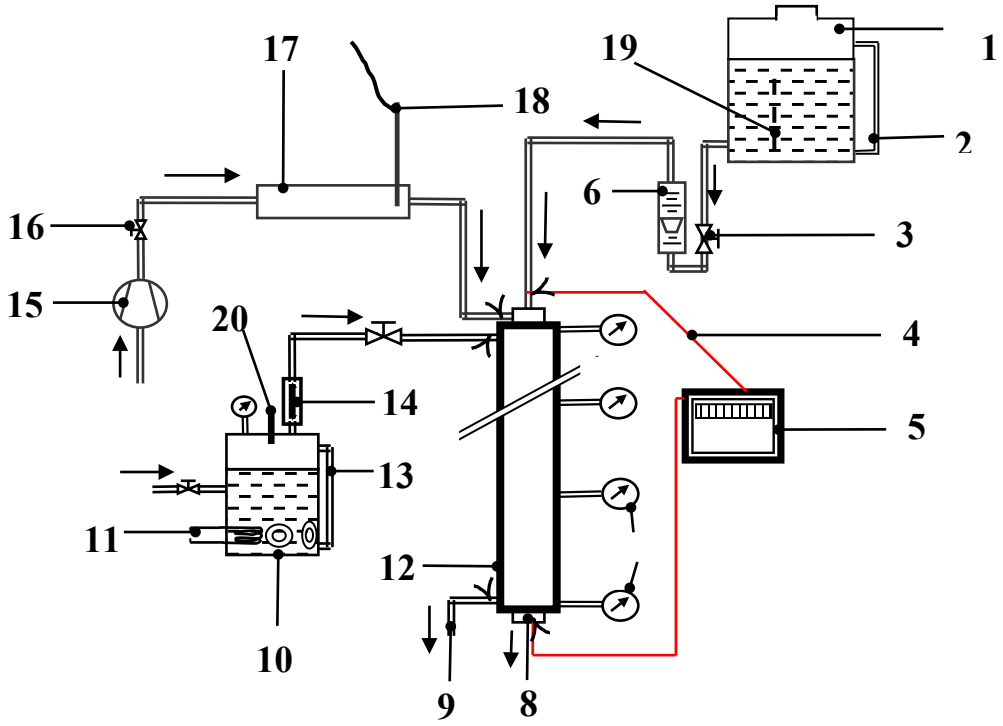

1- Constant head water tank.	8- Two phase flow outlet.	15- Air compressor.
2- Water tank side glass.	9- Condensate outlet.	16-Air regulating valve.
3- Water regulating valve.	10- Electric boiler.	17- Air pipe.
4- Cupper-constantan thermocouple.	11- Electric heater.	18- Hot wire anemometer.
5- Temperature recorder.	12- Test section.	19-Prefarated baffle plate.
6- Water flow meter.	13- Electric boiler side glass.	20-Thermometer.
7- Pressure gauge.	14- Electric super heater.	

Fig. 2. Experimental Test Rig.

Figure (3) shows the details of test section, which consists of three main parts: inner pipe (5), outer sleeve (4), and spherical beads porous medium (7). The inner pipe (5) was manufactured from copper and fixed concentrically inside the outer sleeve (4) by means of 10 cm diameter P.V.C. cap constructing an annulus section.

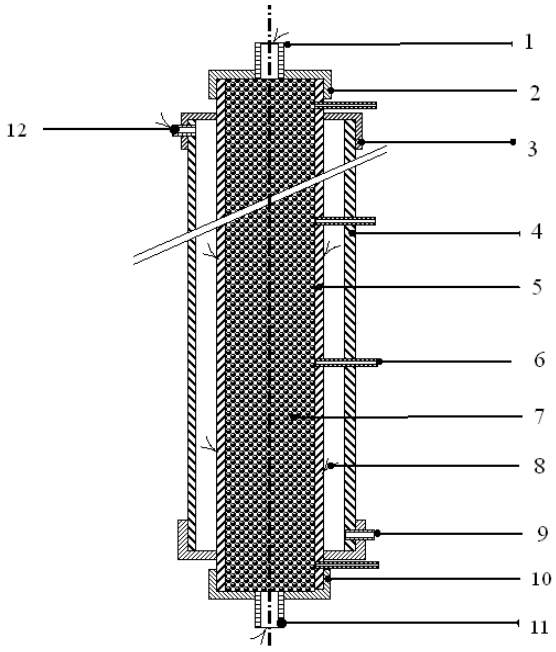

1- Two phase inlet.
2- Teflon connection.
3- P.V.C. cap.
4- Outer cylinder.
5- Copper pipe.
6- Pressure tap.
7- Porous medium.
8- Thermocouple.
9- Condensate outlet.
10- Teflon connection.
11- Two phase outlet.
12- Steam inlet.

Fig. 3. Test Section.

The heat transfer from the wall is gained by the mixture of the two fluids as internal heat capacities: thus,

$$Q = (m_1.c_1 + m_2.c_2).(T_o - T_i) \tag{32}$$

Where, m_1, m_2 are the mass flow rates of water and air respectively; and To and Ti are the temperatures of mixture at outlet and inlet.

The heat transfer coefficient h is given by the equation:

$$h = \frac{Q}{A_s(T_w - T_f)} \tag{33}$$

Where T_w the mean temperature of the cy1inder wall in °C, and T_f is the mean temperature of the fluid in °C, $T_f=(T_i+T_o)/2$. Average Nusselt number Nu_{ex} then can be calculated by

$$Nu_{ex} = \frac{h.r_o}{k_e} \tag{34}$$

VII. Results and Discussion:

To validate the numerical model, experimental pressure drop, temperatures and volume flow rates are measured, and average Nusselt number Nu_a and friction factor f_t at different Reynolds number Re are compared with the corresponding numerical model.

Figure 4 presents the comparison between the experimental and numerical values of the friction factor at different Reynolds number $0.01 \leq Re \leq 500$ for spherical sized packed beads of d=7 mm, $S_l=0.514$. The comparison shows good agreement at Reynolds number up to 100. At Reynolds number Re>100, It is expected for friction factor obtained from the numerical model to deviate from the experimental one. Therefore, Darcy model is only valid for low Reynolds number where inertia effect and friction due to the macroscopic shear are ignored.

VIII. Conclusions:

Heat transfer of two-phase concurrent flow through a vertical, cylindrical, homogeneous porous medium is investigated. The system energy equation and a general form of the Darcy flow model for each phase are the points of interest. The test section is exposed to a constant wall temperature after loaded with spherical beads. The numerical solution of the model is achieved by the finite volume method. The numerical procedure is generalized such that it can be reduced and applied to a single-phase flow model. The numerical results are experimentally validated according to air/water downward flow, spherical beads, a ratio of particle diameter to pipe radius D=0.412, porosity $\varphi=0.396$, $0.01 \leq Re \leq 500$, water to air volume ratio $0 \leq W/A \leq \infty$, and saturation ratio $0 \leq S_l \leq 1$. The main important findings are outlined as follows:

- Average Nusselt number is nearely constant up to Re=40 and increases with the increase of Reynolds number.
- With the increase of Re, the average Nusselt number deviates from the experimental one due to the neglection of inertia and friction effects. The error is about 8% at Re=1000. Therefore, Darcy model is only valid for low Reynolds number.
- At Reynolds number Re>100, It is recommended to take inertia and friction effects into account by means of Forschheimer-Brinkman's equation.
- As X increases from 0 to the end of the thermal entrance length; the mean temperature increases up to a constant value for all Reynolds numbers. θ_m (fully developed) ≈0.67. It also decreases with the increase of Reynolds number at the same section.
- Local Nusselt number has higher values at the entrance section and decreases as X increases until it reaches its fully developed value 4.37 at the end of the thermal entrance length for single phase flow (water or air) and two-phase flow mixture.

- The thermal entrance length X_e is higher for the single-phase flow of the fluid having the higher thermal conductivity "water" and vice versa. For two phase flow mixture, X_e lies between the two previous curves.
- A direct dependence of the thermal entry length on Re, S_1, and properties of the flowing fluids exists and gives a modified correlation for the entrance length; Xe =0.1 Re.Pr.R_m, where $R_m = R_m(S_1, S_2, \rho_1, \rho_2, c_1, c_2)$; which can be compared with that obtained by Poulikakos and Ranken [1] and El-Kady [5] for the single phase flow; $X_e/Pr=0.1$ Re.

IX. Nomenclature:

A	area,	m^2	u	velocity,	m/s
B	Nondimensional pressure gradient.		U	Dimensionless velocity.	
			V	Volume,	m^3
c	specific heat,	J/kg.K	v	volume flow rate,	m^3/s
d	sphere diameter,	m	W/A	Water air ratio.	
D	test section diameter,	m	X	axial coordinate,	m
g	gravity acceleration,	m/s^2	X	dimensionless axial coordinate.	
Ga	Galilio number.		**Greek symbols**		
h	heat transfer coefficient,	W/m^2K	α	thermal diffusivity,	m^2/s
k	thermal conductivity,	W/m K	φ	porosity of the porous medium.	
K	permeability,	m^2			
L	test section length,	m	θ	Dimensionless temperature.	
m	mass flow rate,	kg/s	μ	dynamic viscosity,	kg/m.s
p	pressure,	N/m^2	ν	kinematic viscosity,	m^2/s
Pr	Prandtl number.		ρ	density,	kg/m^3
Q	heat energy,	W			
r	test section radius,	m	**Subscripts:**		
R	nondimensional radius,				
Re	Reynolds number.		1	liquid phase.	
S	Saturation, dimensionless.		2	gas phase.	
T	temperature,	K	3	solid phase.	

a	average.	m	mean.
c	cross section.	o	outer, outlet.
e	entrance.	p	pores.
ef	effective property of the medium.	s	surface.
f	fluid (two phase mixture).	t	total.
i	inlet.	w	wall.

Compliance with Ethical Standards:

No Funding.

Conflict of Interest: The authors declare that they have no conflict of interest. We declare that we have no known competing financial interests or personal relationships that could have appeared to influence the work reported in this paper.

X. References:

1- Poulikakkos, D., and Ranken, K., "Forced convection in a channel filled with porous medium, including the effects of flow inertia, variable porosity, and Brinkman friction", ASME Journal of heat transfer 109 (1987) 880-888.

2- Nield, D., A., and Bejan, A., "Convection in porous media - Fifth Edition", Springer, (2017), https://doi.org/10.1007/978-3-319-49562-0.

3- El Kady, M.S., "A review of fluid and convective heat flow in porous media", Second international Engineering Conference, Mansoura, (1997) 111-123.

4- El Kady, M.S., "Forced convection in a cylindrical porous medium", Second international Engineering Conference, Mansoura, (1997) 125-140.

5- El Kady, M.S., Tolba, M.A. and Rabie, L.H., "Flow in a circular pipe filled with porous medium in the non-Darcian effects", Mansoura Engineering Journal, (20)3 (1995) M1-M18.

6- El Kady, M.S., Tolba, M.A. and Rabie, L.H., "Non-Newtonian behavior of drag reducing fluid flow and heat transfer in a circular pipe filled with porous medium", Mansoura Third International Engineering Conference, (2000) 185-204.

7- Larkins, R.P., "Two phase cocurrent flow in packed beds", Ph.D. dissertation, University of Michigan, (1959).

8- Rao, V.G., Ananth, M.S., and Varma, Y.B.G. "Hydrodynamics of two phase cocurrent downflow through packed beds–Part II. Experiment and correlations"

AICHE Journal, (29)3 (1983) 473-481.

9- Saez, A.E., Carbonell, R.G., and Levec, J., "The hydrodynamics of trickling flow in packed beds- Part II: Experimental observations", AICHE Journal (32)3 (1986) 369-380.

10- Sai, P.S.T., and Varma, Y.B.G., "Pressure drop in gas liquid downflow through packed beds", AICHE Journal (33)12 (1987) 2027-2036.

11- Wang, C.Y., and Beckermann, C, "A two phase mixture model of liquid gas flow and heat transfer in capillary porous media – I. Formulation", Int. J. Heat Mass Transfer (36) (1993) 2747-2758.

12- Rao, V.G., Ananth, M.S., and Varma, Y.B.G. Hydrodynamics of two phase cocurrent downflow through packed beds–Part I. Macroscopic model" AICHE Journal (29)3 (1983) 467-473.

13- Saez, A.E., Carbonell, R.G., and Levec, J., "The hydrodynamics of trickling flow in packed beds- Part I: Conduit models" AICHE Journal, (32)3 (1986) 353-368.

14- Hilfer, R., "Macroscopic equations of motion for two phase flow in porous media", The American Physical Society, Physical Review E, (58)2 (1998) 2090-2096.

15- Carbonell, R. G., Multiphase models in packed beds", Oil & Gas Science and Technology- Rev. IFP (55) 4 (2000) 417-425.

16- Starikovicius, V., "The multiphase flow and heat transfer in porous media" Vilnius Gediminas Technical University, Computing center, LT-2040, Lithuania, (2003).

17- Binning, P.J, "Modeling unsaturated zone flow and contaminant transport in the air and water phases" Ph.D. dissertation, Faculty of Princeton university, Civil engineering department., (1994).

18- Durlofsky, L., J., "Coarse scale models of two-phase flow in heterogeneous reservoirs: volume averaged equations and their relationship to existing upscaling techniques.", Computational Geosciences 2 (1998) 73-92.

19- Juanes, R. and Patzek, T.W., "Relative permeabilities in co-current three phase displacements with gravity.", Society of Petroleum Engineers, 83445, (2003).

20- Marle, C., M., "Multiphase flow in porous media", Gulf, Houston, (1981).

21- Julia, C. Muccino, William, G. Gray, Lin, A. Ferrand, "Toward an improved understanding of multi-phase flow in porous media", Reviews of Geophysics (36)3 (1998) 401-422.

22- Niessner, J., Hassanizadeh, S.M., "A model for two-phase flow in porous media

including fluid-fluid interfacial area", Water resources research, 44(2008) W08439 1-10.

23- Sergio Rojas, Joel Koplik, "Nonlinear flow in porous media", Physical Review (58)4 (1998) 4776-4782.

24- Tore, I. Bjørnarå, NGI, Norway, Eyvind, Aker, "Comparing equations for two-phase fluid flow in porous media", Excerpt from the Proceedings of the COMSOL Conference-Hannover, (2008).

25- Jennifer Niessner, "The role of interfacial areas in two-phase flow in porous media–bridging scales and coupling models", Der Fakult¨at Bau-und Umweltingenieurwissenschaften und dem Exzellenzcluster Simulation Technology der Universit¨at Stuttgart, PhD. Thesis (2010).

26- Ali, Q. Raeini, Martin, J. Blunt, Branko Bijeljic, "Modelling two-phase flow in porous media at the pore scale using the volume-of-fluid method", Journal of Computational Physics 231 (2012) 5653–5668.

27- Bertrand Lagree, "Modelling of two-phase flow in porous media with volume-of-fluid method". Mechanics [physics]. Universit_e Pierre et Marie Curie-Paris VI PhD. Thesis (2015).

28- Michel Quintard, "Introduction to Heat and Mass Transport in Porous Media, Science and Technology", Public Release, STO-EN-AVT-261 (2016) 1-42.

29- Sylvain Pasquier, Michel Quintard, and Yohan Davit, "Modeling two-phase flow of immiscible fluids in porous media: Buckley-Leverett theory with explicit coupling terms". Physical Review Fluids (2)10 (2017) 104101/1-104101/19. ISSN 2469-990X

30- Yangyang, Qiao, Huanyao, Wen, Steinar, Evje, "Compressible and viscous two-phase flow un porous media based on mixture theory formulation", American Institute of Mathematical Sciences, (14)3 (2019) 489-536.doi:10.3934/nhm.2019020

31- Lili, Wang, Yunliang, Li, Guizhang, Zhao, Nanxiang, Chen, Yuanzhi, Xu, "Experimental investigation of flow characteristics in porous media at low Reynolds numbers (Re→0) under different constant hydraulic heads' Water (11)11 (2019) 2317. https://doi.org/10.3390/w11112317

32- Francisco, J. Carrillo, Ian, C. Bourg, Cyprien, Soulaine, "Multiphase flow modeling in multiscale porous media: An open-source micro-continuum approach", Journal of Computational Physics: X 8 (2020) 100073.

33- Yangyang, Qiao, Steinar, Evje, "A compressible viscous three-phase model for

porous media flow based on the theory of mixtures", Advances in Water Resources 141 (2020) 103599.

34- Qiao, Y., Andersen, P.O., Evje, S., Standnes, D.C., "A mixture theory approach to model co- and counter-current two-phase flow in porous media accounting for viscous coupling", Adv. Water Resour., 112 (2018) 170–188.

35- André Baumann, Dennis Hoch, Jens Behringer, Jennifer Niessner, "Macro-scale modeling and simulation of two-phase flow in fibrous liquid aerosol filters", Engineering Applications of Computational Fluid Mechanics, (14)1 (2020) 1325-1336. DOI: 10.1080/19942060.2020.1828174

36- Mays Subhi Sadeq and Zena Khalefa Kadhim, "The effect of container shape and porous media on heat transfer", Journal of Mechanical Engineering Research and Developments CODEN: JERDFO (43)6 (2020) 197-206. ISSN: 1024-1752.

37- Patankar, S., "Numerical heat transfer and fluid flow," Mc Graw Hill,New York, (1980).

38- Versteeg, H.K., and Malalasekera, W., "An introduction to computational fluid dynamics the finite volume method," John Wiley & Sons Inc., New York, (1995).

39- Dally, J.W., Riley, W.F., McConnell, K.G., "Instrumentation for engineering measurements" John Wiley & Sons Inc., New York, (1993).

Figures

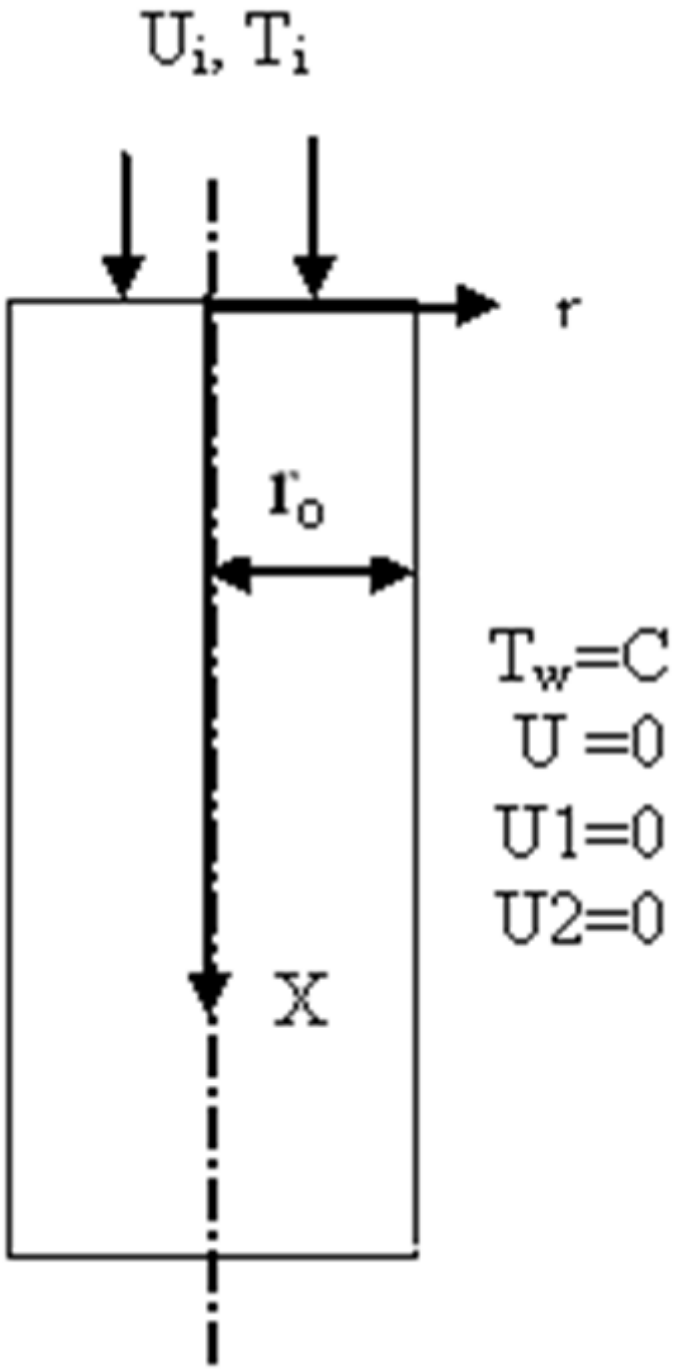

Figure 1

Physical model, coordinate system and boundaries.

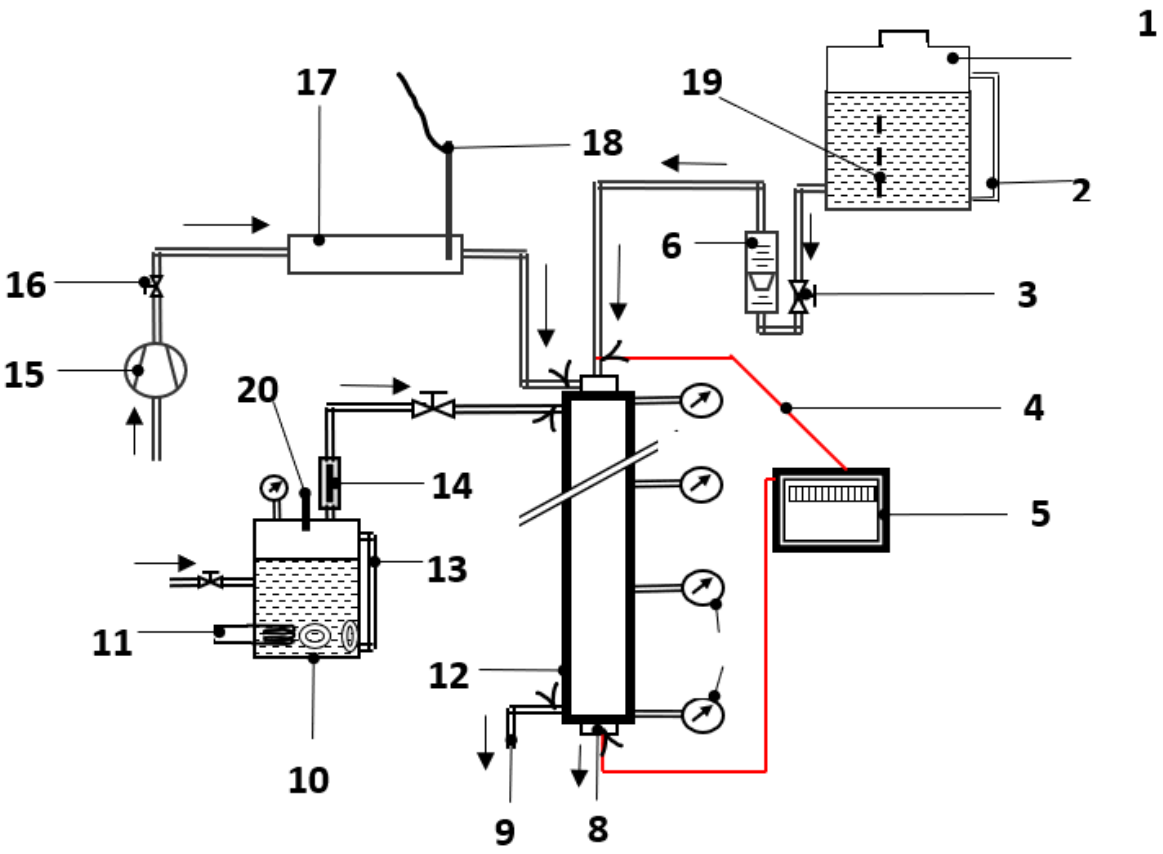

1- Constant head water tank.	8- Two phase flow outlet.	15- Air compressor.
2- Water tank side glass.	9- Condensate outlet.	16-Air regulating valve.
3- Water regulating valve.	10- Electric boiler.	17- Air pipe.
4- Cupper-constantan thermocouple.	11- Electric heater.	18- Hot wire anemometer.
5- Temperature recorder.	12- Test section.	19-Prefarated baffle plate.
6- Water flow meter.	13- Electric boiler side glass.	20-Thermometer.
7- Pressure gauge.	14- Electric super heater.	

Figure 2

Experimental Test Rig.

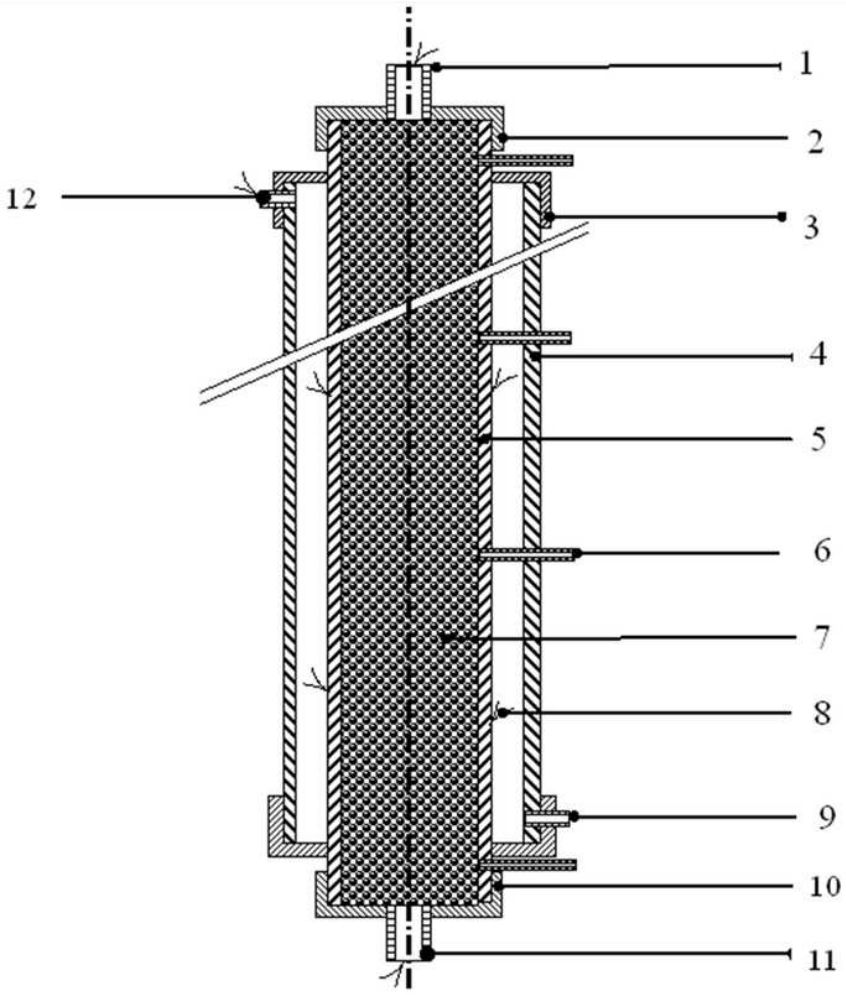

1- Two phase inlet.
2- Teflon connection.
3- P.V.C. cap.
4- Outer cylinder.
5- Copper pipe.
6- Pressure tap.
7- Porous medium.
8- Thermocouple.
9- Condensate outlet.
10- Teflon connection.
11- Two phase outlet.
12- Steam inlet.

Figure 3

Test Section.